

# The Role of AMACR, CD10, TMPRSS2-ERG, and p27 Protein Expression Among Different Gleason Grades of Prostatic Adenocarcinoma on Needle Biopsy

Clinical Medicine Insights: Oncology  
Volume 14: 1–8  
© The Author(s) 2020  
Article reuse guidelines:  
sagepub.com/journals-permissions  
DOI: 10.1177/1179554920947322



Özdemir Gülhan<sup>1</sup>  and Balcı Mahi<sup>2</sup> 

<sup>1</sup>Department of Pathology, Mengücek Gazi Training and Research Hospital, Erzincan Binali Yıldırım University, Erzincan, Turkey. <sup>2</sup>Department of Pathology, Faculty of Medicine, Kirikkale University, Kirikkale, Turkey.

## ABSTRACT

**OBJECTIVE:** We examined the immunohistochemical expression of  $\alpha$ -methyl acyl coenzyme A racemase (AMACR), CD10, TMPRSS2-ERG, and p27 in prostate adenocarcinoma tumors with different Gleason growth patterns and nonneoplastic prostate tissues to elucidate their roles in prostate carcinogenesis and histological aggressiveness.

**MATERIAL AND METHODS:** In total, 80 archival core biopsy tissues diagnosed as prostate carcinoma, benign prostate hyperplasia, and atrophy cases were included. Immunoreactivity was evaluated by calculating the percentage of positively stained cells and the staining intensity. The mean values and test of significance were obtained using the Kruskal-Wallis test.

**RESULTS:** We obtained mostly intense immunoreactivity for AMACR, CD10, and ERG in adenocarcinomas. Although no significant differences were noted regarding AMACR and ERG expression, samples with Gleason growth patterns 3 and 5 tended to be strongly positive for ERG. Pattern 3 tumors exhibited the weakest positivity for CD10. The p27 expression was strong and diffuse in nonneoplastic prostate tissues. The loss of p27 expression was more frequent for pattern 5 tumors.

**CONCLUSION:** ERG and AMACR were powerful markers to detect cancer. Especially, ERG is evident in early tumors may reflect its interaction with functional androgen receptors in cancer initiation. Pattern 5 tumors associated with stroma may have been exposed to more stromal substrates and upregulate their CD10 content as a protein degrader. We suggest that CD10 expression is associated with an increasing tumor grade. Decreased concentrations of p27 protein might be implicated in prostate carcinogenesis and may be a useful immunohistochemical adjunct in predicting histological aggressiveness.

**KEYWORDS:** Prostate adenocarcinoma, Gleason score, AMACR, CD10, TMPRSS2-ERG, p27

**RECEIVED:** April 18, 2020. **ACCEPTED:** July 6, 2020.

**TYPE:** Original Research

**FUNDING:** The author(s) disclosed receipt of the following financial support for the research, authorship, and/or publication of this article: This study was supported by the Kirikkale University Scientific Research Projects Unit with project code number 2018/073.

**DECLARATION OF CONFLICTING INTERESTS:** The author(s) declared no potential conflicts of interest with respect to the research, authorship, and/or publication of this article.

**CORRESPONDING AUTHOR:** Özdemir Gülhan, Department of Pathology, Mengücek Gazi Training and Research Hospital, Erzincan Binali Yıldırım University, Erzincan, Merkez 24100, Turkey. Email: drgozdemir@gmail.com

## Introduction

A major challenge in the treatment of prostate carcinoma is discriminating aggressive tumors related to high mortality rates from their indolent forms, which are less likely to cause harm in patients. To stratify patients into risk groups, a wide variety of screening tools or biomarkers are routinely used in practice. However, there is a lack of reliable and reproducible assays to determine tumor behavior.

Diagnosis of prostate adenocarcinoma mainly depends on the histopathological evaluation of trans-rectal ultrasound-guided biopsy specimens after the detection of elevated serum prostate-specific antigen (PSA) levels, 1 of the first-choice biomarkers. Although the histopathological diagnosis of prostate adenocarcinoma is easy in most cases, early detection of the disease makes it more challenging for pathologists to assess small foci with atypical glands. Immunohistochemical markers have become necessary tools to confirm the diagnosis in such cases. When the diagnosis of carcinoma is assured, estimation of the Gleason score, which is an extremely important predictor of tumor progression, should be performed.

In this study, we investigated a number of biomarkers that both strengthened the diagnosis and indicated the aggressiveness of the lesions. The identified biomarkers included  $\alpha$ -methyl acyl coenzyme A racemase (AMACR), an enzyme involved in the peroxisomal  $\beta$ -oxidation of branched chain fatty acids and their derivatives. In prostatic adenocarcinoma, AMACR is overexpressed at both the RNA and protein levels. However, AMACR expression has been frequently reported in prostatic intraepithelial neoplasia and to varying degrees in benign prostatic glandular epithelium. Therefore, in clinical pathology, AMACR staining is combined with basal cell markers such as p63 and 34 $\beta$ E12, which are not expressed in prostate adenocarcinoma.<sup>1</sup>

Another marker included in our study was CD10, a 100-kDa transmembrane glycoprotein also known as neutral endopeptidase or enkephalinase. The biological functions of CD10 substrates in prostate tissue are not fully understood. Proenkephalin, which is expressed by prostate stromal fibromuscular cells, may be a substrate for CD10. CD10 is strongly expressed by normal prostatic luminal epithelial cells, whereas



Creative Commons Non Commercial CC BY-NC: This article is distributed under the terms of the Creative Commons Attribution-NonCommercial 4.0 License (<https://creativecommons.org/licenses/by-nc/4.0/>) which permits non-commercial use, reproduction and distribution of the work without further permission provided the original work is attributed as specified on the SAGE and Open Access pages (<https://us.sagepub.com/en-us/nam/open-access-at-sage>).

decreased expression of CD10 was suggested to correlate with a more aggressive phenotype with greater malignant potential. Moreover, loss or decreased expression of CD10 is claimed to be an early and frequent event in human prostate cancer.<sup>2,3</sup>

The most common genetic alteration, being reported in 50%-70% of patients with prostate carcinoma, is the *TMPRSS2-ERG* fusion gene, in which the promoter of transmembrane protease, serine 2 (*TMPRSS2*) is fused with the coding sequence of erythroblastosis virus E26 (Ets) gene family members.<sup>4</sup> ERG expression has been reported to be associated with advanced tumor stage, high Gleason scores, and metastasis.<sup>5</sup> In addition, ERG positivity in needle biopsy samples is used in the differential diagnosis of lesions mimicking carcinoma, but the additional value of p63, basal cell keratin 5, and other markers such as AMACR is limited.<sup>6</sup>

The last marker we used was tumor suppressor p27<sup>Kip1</sup>, a cyclin-dependent kinase inhibitor. Decreased immunohistochemical expression of p27<sup>Kip1</sup> is associated with tumor progression and poor prognosis in many neoplasms such as breast, colorectal, and lung carcinomas.<sup>7</sup> It is known that PTEN (phosphatase and tensin homolog) loss increases with Gleason grade, and various studies in prostate carcinoma indicated that p27, which is inactivated by PTEN loss, is silenced or degraded as the Gleason score increases. However, some reports failed to find any correlation with clinical outcome or aggressive parameters.<sup>7,8</sup>

This study compared the expression of these markers between nonneoplastic prostate tissues and cancer tissue and assessed their levels in different Gleason patterns, which reflect tumor behavior.

## Materials and Methods

### Patients

This study included 80 patients who were diagnosed with prostate adenocarcinoma, benign prostatic hyperplasia, and prostatic atrophy via prostate needle biopsy between 2006 and 2019 at the Pathology Department of Kirikkale Medical School. The carcinoma cases were divided into 3 categories according to their Gleason patterns (patterns 3-5) according to the 2014 International Society of Urological Pathologist consensus criteria.<sup>9</sup> Prostatic hyperplasia and atrophy comprised the control groups. Clinical information was obtained from hospital automation system and patient files. Written informed consent was obtained from all subjects before the study.

### Immunohistochemical procedures

An immunohistochemical study was performed on 4 µm sections of dewaxed and dehydrated formalin-fixed, paraffin-embedded tissues. After heat-induced antigen retrieval, slides were processed using the BenchMark Autostainer (Ventana Medical Systems Inc, Tucson, AZ, USA) using the Ultraview DAB detection kit (Ventana Medical Systems Inc) according

to the manufacturer's instructions. The following prediluted monoclonal antibodies were used in all cases: p27<sup>Kip1</sup> (clone SX53G8; Dako Ltd, Ely, UK), CD10 (clone SP67; Ventana), AMACR/anti-p504s (clone SP116; Ventana), and ERG (clone EPR 3864; Epitomics, Burlingame, CA, USA).

### Evaluation of immunohistochemical staining

Immunoreactivity of the antibodies was scored using a semi-quantitative scoring method based on both the proportion of positively stained tumor cells and the staining intensity of tumor cells. The expression of each protein was evaluated by calculating the total immunoreactive score (IRS) as the product of the ratio and intensity scores. The proportion score reflected the estimated fraction of positive-stained tumor cells (0, none; 1, 1%-10%; 2, 11%-50%; 3, 51%-80%; and 4, 81%-100%). The intensity score represented the estimated staining intensity (0, no staining; 1, weak; 2, moderate; and 3, strong). The total IRS ranged from 0 to 12, and the scores were averaged. Positive expression was defined as an averaged score exceeding the median for each antibody.

### Statistical analysis

SPSS 25.0 (IBM Corporation, Armonk, NY, USA) was used to analyze the variables. We performed Kolmogorov-Smirnov and Levene tests to assess the differences in the distribution and variance of samples in each group. One-way analysis of variance (robust statistic: Brown-Forsythe) and Tukey HSD test were used to compare the groups according to age, and the Kruskal-Wallis *H* test for nonparametric methods was used to compare the groups regarding PSA, AMACR, CD10, ERG, and p27 expression. The Monte Carlo simulation technique was used with the results, and Dunn test was used for post hoc analysis. Quantitative variables are presented as the mean ± SD (minimum/maximum) or median (minimum/maximum), whereas categorical variables are presented as n (%). The variables were examined at the 95% confidence level, and *P* < .05 denoted significance.

## Results

Table 1 presents the age distribution and PSA levels of patients and the frequencies of AMACR, CD10, ERG, and p27 expression in the control and tumor Gleason pattern groups. PSA levels were significantly higher in the pattern 5 group than in the other groups. However, the mean age was highest in the pattern 4 group.

AMACR expression was only detected in 1 patient in the control group who had an IRS of 4 (Figure 1A). No gene expression was detected in the other 19 patients. We detected slightly more immunopositive cases in pattern 3 than in patterns 4 and 5. However, no significant differences in terms of AMACR expression were observed among the tumor patterns (Figure 1A and C).

**Table 1.** Distribution of cases according to clinical variables and immunohistochemical staining scores.

|                     |          | AGE                      | PSA                         | AMACR                       | CD10                    | ERG                         | P27                         |
|---------------------|----------|--------------------------|-----------------------------|-----------------------------|-------------------------|-----------------------------|-----------------------------|
|                     |          | MEAN $\pm$ SD (MIN/MAX)  | MEDIAN (MIN/MAX)            | MEDIAN (MIN/MAX)            | MEDIAN (MIN/MAX)        | MEDIAN (MIN/MAX)            | MEDIAN (MIN/MAX)            |
| Control             | C (n=20) | 64.65 $\pm$ 8.40 (50/84) | 4.21 (2.40/6.78)            | 0 (0/4)                     | 4 (2/8)                 | 0 (0/0)                     | 9 (3/12)                    |
| Pattern III         | 3 (n=20) | 63.95 $\pm$ 7.67 (49/77) | 8.08 (4.11/37.58)           | 12 (0/12)                   | 2 (0/8)                 | 5.5 (0/12)                  | 4 (0/12)                    |
| Pattern IV          | 4 (n=20) | 73.70 $\pm$ 9.25 (55/89) | 27.86 (4.56/154)            | 10.5 (4/12)                 | 4 (0/8)                 | 1.5 (0/12)                  | 4 (2/9)                     |
| Pattern V           | 5 (n=20) | 68.20 $\pm$ 7.16 (56/79) | 80.26 (3.87/100)            | 10 (0/12)                   | 4 (0/12)                | 4.5 (0/12)                  | 2 (0/9)                     |
| <i>P</i> value      |          | <b>.001<sup>a</sup></b>  | <b>&lt;.001<sup>b</sup></b> | <b>&lt;.001<sup>b</sup></b> | <b>.004<sup>b</sup></b> | <b>&lt;.001<sup>b</sup></b> | <b>&lt;.001<sup>b</sup></b> |
| Pairwise comparison | C→III    | 0.993                    | <b>0.014</b>                | <b>&lt;0.001</b>            | <b>0.011</b>            | <b>0.001</b>                | <b>0.002</b>                |
|                     | C→IV     | <b>0.004</b>             | <b>&lt;0.001</b>            | <b>&lt;0.001</b>            | 0.999                   | <b>0.002</b>                | <b>&lt;0.001</b>            |
|                     | C→V      | 0.518                    | <b>&lt;0.001</b>            | <b>&lt;0.001</b>            | 0.999                   | <b>0.001</b>                | <b>&lt;0.001</b>            |
|                     | III→IV   | <b>0.002</b>             | <b>0.021</b>                | 0.999                       | <b>0.010</b>            | 0.999                       | 0.999                       |
|                     | III→V    | 0.359                    | <b>0.036</b>                | 0.999                       | <b>0.001</b>            | 0.999                       | 0.272                       |
|                     | IV→V     | 0.152                    | 0.927                       | 0.999                       | 0.999                   | 0.999                       | 0.817                       |

Abbreviations: AMACR,  $\alpha$ -methyl acyl coenzyme A racemase; Min: Minimum; Max: Maximum; PSA, prostate-specific antigen.

<sup>a</sup>Univariate analysis of variance (Robust Statistic: Brown-Forsythe); post hoc test: Tukey HSD; <sup>b</sup>Kruskal-Wallis *H* test (Monte Carlo); post hoc test: Dunn test. *P* values-set in boldface indicate statistical significance.

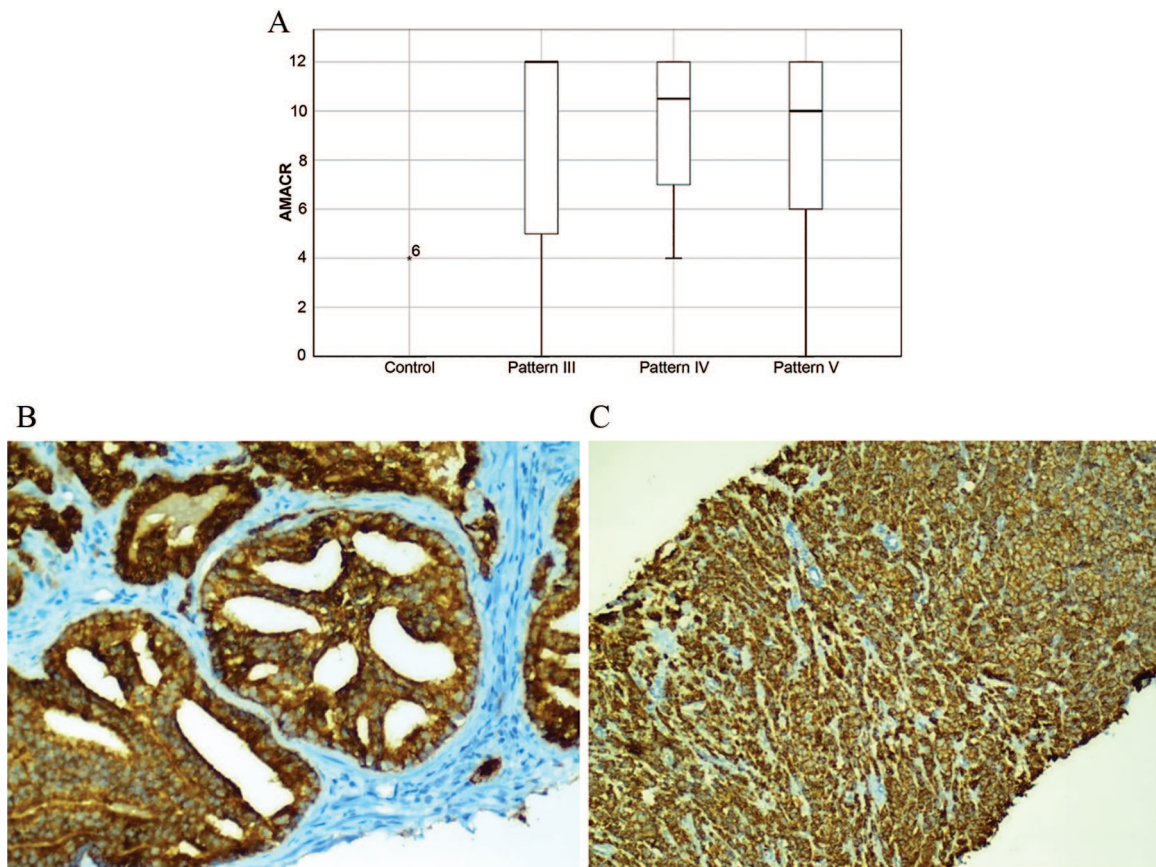


**Figure 1.** (A) Box plot presentation of immunohistochemical AMACR staining in nonneoplastic prostate and carcinoma cases with different Gleason growth patterns. No staining was performed, except for 1 case in the control group. The strongest staining tended to accumulate in pattern 3. Plots were scaled by dividing each median value. (B and C) Strong staining for  $\alpha$ -methyl acyl coenzyme A racemase was observed in pattern 4 and 5 tumors.

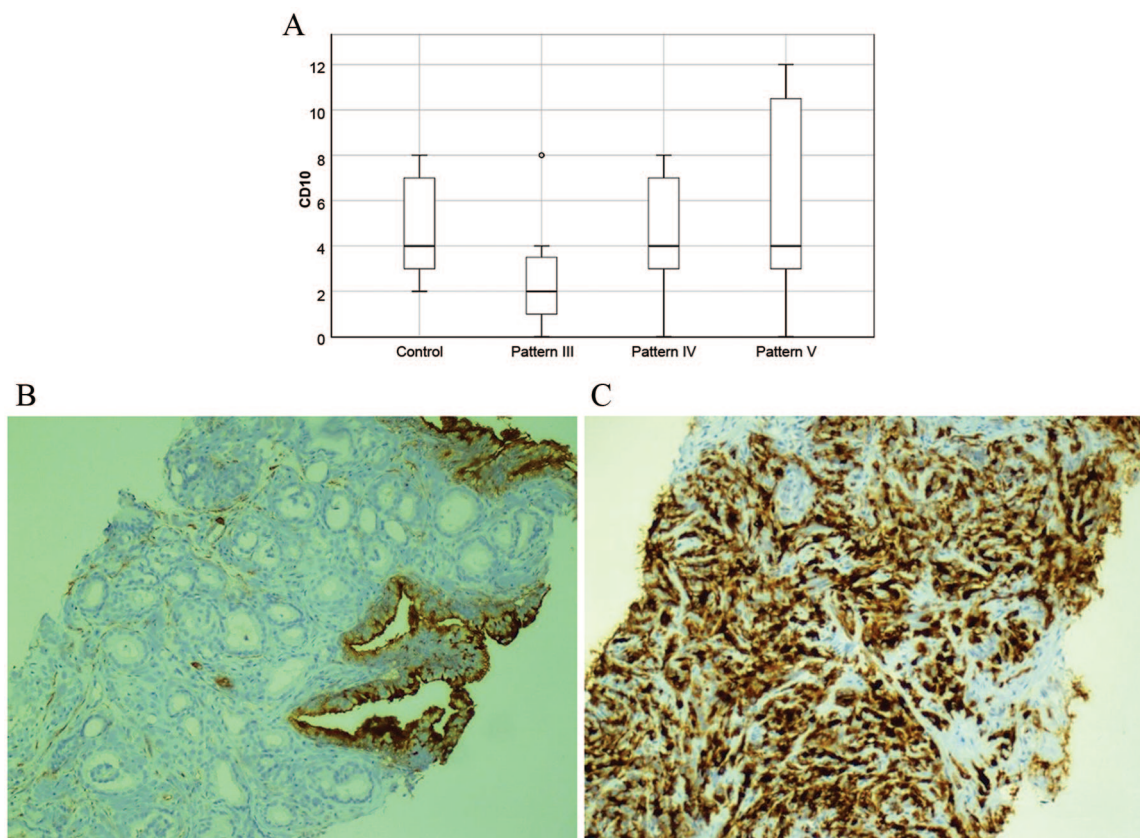


**Figure 2.** (A) Box plot for CD10 expression demonstrated pattern 3 cases showed the least staining intensity. CD10 was more abundantly expressed in pattern 5 than the other patterns. Plots were scaled by dividing each median value. (B) Most pattern 3 tumors did not express CD10, whereas hyperplastic glands exhibited luminal staining for CD10. (C) Pattern 5 tumors displayed diffuse strongly positive cytoplasmic staining for CD10.

CD10 expression varied among the groups. Among the groups, pattern 3 tumors had the lowest tendency to be stained with this antibody (Figure 2A). Luminal expression was significant in nonneoplastic prostatic tissues and low-grade pattern 3 carcinomas (Figure 2B). Slit-like immunoreactivity was observed in Gleason grade 4 tumors, whereas cytoplasmic staining was dominant in grade 5 tumors (Figure 2C).

None of the patients exhibited immunoreactivity for ERG in the control group (Figure 3A). Higher staining scores were obtained in patterns 3 and 5 than in pattern 4 (Figure 3B and C). However, there were significant differences among the tumor grades.

The p27 expression was strong and diffuse in nonneoplastic prostate tissues. In addition, its expression was significantly different between the control and tumor groups (Figure 4A). The p27 expression was moderately or weakly positive in patients with adenocarcinoma in higher pattern groups (Figure 4B). We observed the loss of expression more frequently in pattern 5 patients (Figure 4C).

## Discussion

Following recent advances in understanding the molecular pathways associated with prostate carcinoma, new biomarkers with prognostic and diagnostic potential have been developed. The diagnosis of prostate adenocarcinoma is based on a

combination of cytological and architectural histopathological features. However, it is important to support the diagnosis using other methods because histopathological examination alone makes interpretation difficult because prostate carcinoma mimics conditions such as adenosis and atypical adenomatous hyperplasia. Therefore, immunohistochemistry plays a crucial role in the diagnostic pathology of the prostate, particularly in the diagnosis of minute prostate adenocarcinoma. Basal cell markers such as HMWCK (34 $\beta$ E12), cytokeratins 5/6, and p63 are extremely useful for identifying basal cells, and their presence argues against a diagnosis of invasive prostate carcinoma. Basal cell markers, while helpful, basal cell staining can be discontinuous that cause to be interpreted as negative in cases of benign prostate tumors, adenosis, or prostatic atrophy; thus, new sensitive and specific immunohistochemical markers will aid in increasing the level of confidence in establishing a definitive diagnosis of malignancy in prostate pathology.

In this study, we evaluated AMACR, CD10, TMPRSS2-ERG, and p27 protein expression in nonneoplastic prostate tissues and adenocarcinoma tissues with different Gleason growth patterns. We focused mainly on histopathological tumor patterns that correlated well with tumor aggressiveness and the areas of atrophy in benign prostate tissue that could be mistaken for malignancy.

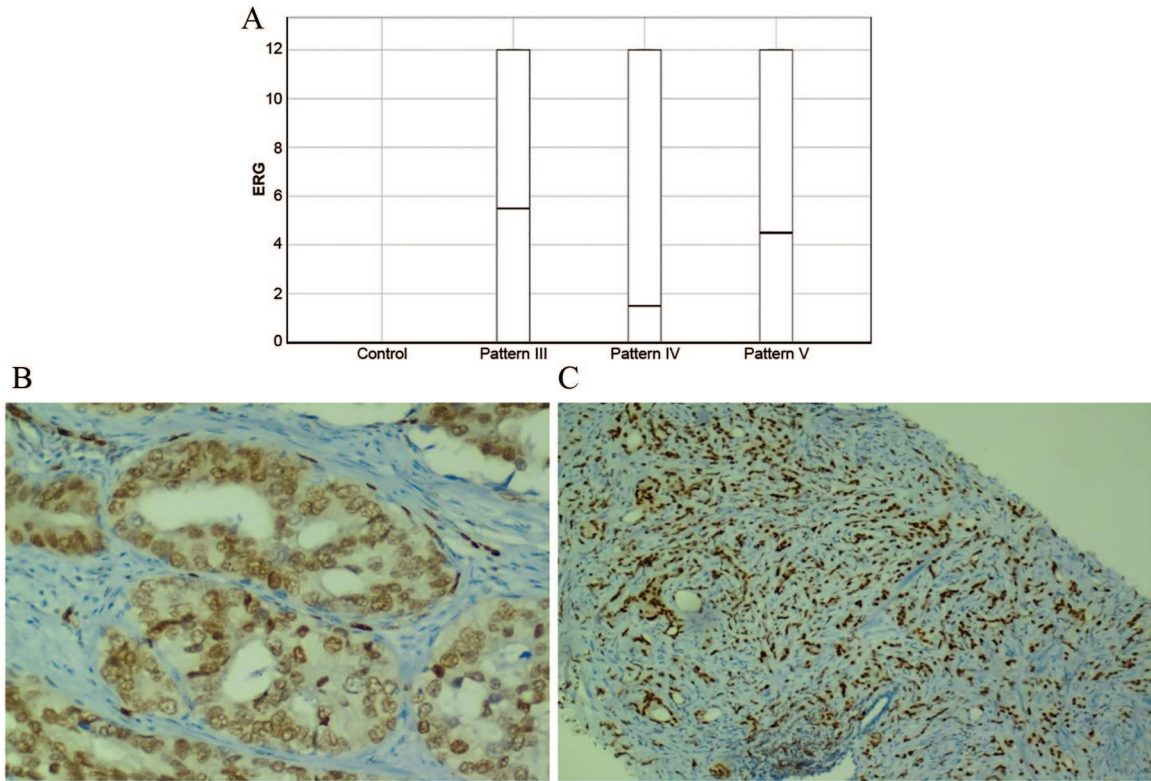


**Figure 3.** (A) Box plot for ERG expression. No immunopositivity was detected in nonneoplastic prostate tissues. Plots were scaled by dividing each median value. (B) Weak ERG positivity in a pattern 4 tumor. (C) Intense nuclear staining for ERG in a pattern 5 tumor.

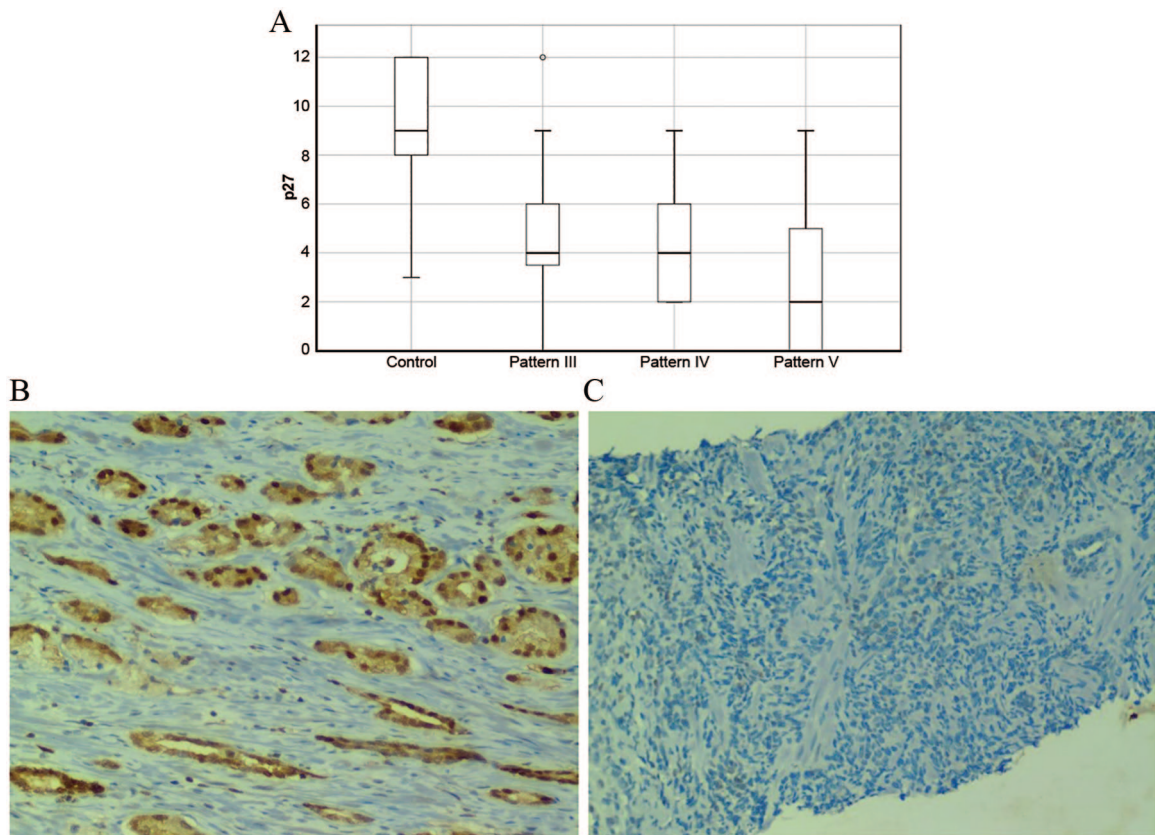


**Figure 4.** (A) Box plot for p27 staining. Decreased expression was noted among carcinoma cases because strong immunoreaction was evident in the control group. Plots were scaled by dividing each median value. (B) Pattern 3 glands exhibit strong nuclear positivity for p27. (C) No p27 staining was found in pattern 5 tumors.

Initial immunohistochemical studies of AMACR revealed that the protein was nearly 100% specific and sensitive for prostate carcinoma, whereas benign glands only exhibited poor apical staining or no expression.<sup>10,11</sup> However, in later studies, AMACR expression was reported in benign conditions such as atypical glandular proliferation, intraepithelial premalignant lesions, and prostatic atrophy.<sup>12</sup> In our study, we identified 4 cases of poor luminal AMACR staining in nonneoplastic prostate tissues in accordance with the literature. But we expected that all cancer cases must be strongly stained with this biomarker; however, unpredictable decreases or increases in expression are observed. According to a study by Murphy et al, 38% of carcinomas exhibited heterogeneous AMACR expression, and this expression pattern was most commonly observed in carcinomas with Gleason scores of  $\geq 7$ . There was a significant correlation between heterogeneous AMACR expression and higher Gleason scores.<sup>13</sup> We can suppose that glandular lumen formation, which is the only indicator of differentiation, is associated with racemase activity, as observed in colorectal carcinomas.<sup>14</sup> AMACR downregulation is claimed to be a process of dedifferentiation, and another explanation for this heterogeneity is that some new malignant clones use the central macronutrient glucose rather than energy sources obtained from the  $\beta$ -oxidation of fatty acids. The prostate gland is exquisitely sensitive to androgenic hormones. Androgens influence both the synthesis and uptake of fatty acids in prostate cells, but prostate epithelial cells exhibit high rates of aerobic glycolysis and low rates of oxidative phosphorylation under normal circumstances. During malignant transformation, prostate cancer lines exhibit increased oxidative phosphorylation and reactivation of the citric acid cycle to oxidize citrate for energy production. De novo lipogenesis is enhanced at this stage of disease through the upregulation of androgen-regulated lipogenic enzymes.<sup>15</sup> Unfortunately, most tumors eventually become androgen-independent via mutations or epigenetic changes that activate alternative signaling pathways while switching the lipogenic phenotype to a Warburg effect-dominant type.

Another marker examined in this study was CD10, a luminal cell marker of which expression is directly in the apical surface of glandular lumen. It plays a role in the inactivation of certain peptide hormones, such as enkephalin, bombesin, and substance P, which influence growth, angiogenesis, invasiveness, and metastasis. CD10 reduces the local concentration of these peptides available for receptor binding and signal transduction. It has been suggested that the loss or downregulation of CD10 expression accelerates tumor development or progression. Early loss of CD10 expression has been reported in a high percentage of prostate tumors.<sup>2,3</sup> In this study, pattern 3 tumors had the lowest rate of CD10 positivity among the various Gleason pattern and control groups. In accordance with the findings of Kaur et al,<sup>16</sup> mostly membranous and apical staining was observed in pattern 3 or benign hyperplastic glands, compared with more cytoplasmic staining in pattern 4

and 5 foci. Tawfic et al<sup>17</sup> reported an absence of CD10 expression in Gleason grade 2 and 3 tumors but noted high cytoplasmic and membranous CD10 expression in high Gleason grade tumors. The decline in CD10 expression in low-grade tumors may be explained by the loss of the tumor-suppressive effect of this endopeptidase, but it remained located predominantly on the luminal aspect of tumor cells and acted as a surface enzyme to hydrolyze different peptides. We believe that the cytoplasmic localization of CD10 occurs when luminal formation becomes difficult, as observed in pattern 5, in which tumor cells proliferate as invasive, solid spheres or as single cells. Changes in the localization of CD10 may also change its biological function. The CD10-positive subpopulation in head and neck squamous cell carcinomas has been reported to acquire cancer stem cell properties and express higher levels of OCT3/4.<sup>18</sup> Conversely, pattern 5 cancer cells associated with the stroma may have been exposed to more stromal substrates, leading to the upregulation of CD10 as a proteolytic enzyme. Although the exact mechanism is unclear, we suggest that CD10 expression appears to be associated with increasing tumor grade.

In this study, we explored the expression pattern of *TMPRSS2-ERG*, which was overexpressed in 55% of prostate cancer cases in a study published in 2005.<sup>4,19</sup> *ERG* is an oncogene that regulates embryonic development, cell proliferation, differentiation, angiogenesis, inflammation, and apoptosis. Androgen-induced fusion of the promoter region of *TMPRSS2* and *ERG* genes was mostly observed in prostate cancer. Numerous studies evaluated the significance of *TMPRSS2-ERG* in prostate cancer with varying results. Based on our data, *ERG* is a malignancy marker because we did not observe its immunopositivity in nonneoplastic prostate tissues. However, there was no statistically significant relationship between Gleason patterns and *ERG* overexpression. Our data were similar to the findings of Liu,<sup>20</sup> Font-Tello et al,<sup>21</sup> and Wang et al.<sup>22</sup> However, strong *TMPRSS2-ERG* expression was noted in Gleason pattern 3 and 5 tumors in our study. Lee et al<sup>23</sup> reported that *ERG* expression was higher in tumors with low Gleason scores, but as noted in our study, statistical significance was not achieved because of the small sample size. In the same study, *ERG* expression was negative in all other benign conditions mimicking malignancy. In a study by Nie et al, high *ERG* protein expression was observed in patients with low Gleason scores. In their report, the pattern 3 areas exhibited positive *ERG* staining in 8 of 27 radical prostatectomy cases, whereas the pattern 4 areas of the same patients were stained negatively.<sup>24</sup> Studies have indicated that *TMPRSS2-ERG* fusion may be an early molecular change in tumors with lower Gleason scores, contradicting other studies indicating that the fusion gene is associated with a more aggressive prostate cancer phenotype.<sup>25-28</sup> As we mentioned previously, prostate cancers exhibit intratumor heterogeneity, similarly as other cancer types. Thus, these different results are acceptable when we consider the androgen status of patients because androgen

stimulates *TMPRSS2* expression. In another scenario, considering the age at which pattern 5 tumor growth occurs, we can argue that some proliferation patterns reflect a de novo clone with a sudden outgrowth inside or near a tumor with a lower Gleason grade without a stepwise continuum of well-differentiated glands to fused glands, as observed in Gleason grade 4. ERG may be overexpressed as long as androgen is abundant in the environment, as observed in early-grade tumors. Therefore, it may be possible to predict which tumors will still respond to androgen castration. This may determine the tumor response to inhibition of ERG expression.

It is believed that the progression from hormone-dependent to hormone-independent prostate tumor growth involves a cascade of genetic changes reflected, eg, by the activation of oncogenes such as Bcl-2 and c-Myc or the inhibition of tumor suppressor genes such as p53 and PTEN. Low tumor suppressor gene expression is expected to be a poor prognostic signal indicating decreased apoptotic and increased proliferative activity.<sup>29</sup> Unlike other cyclin-dependent kinase-inhibitory genes, the p27<sup>Kip1</sup> gene is rarely mutated in carcinomas but is inactivated through impaired synthesis, accelerated degradation, and mislocalization.<sup>30,31</sup> In this study, loss of p27 was associated with tumors with high Gleason grades. A number of studies proposed that tumors with lost or diminished p27 expression are more aggressive, whereas other studies found no such correlation or even reported inverse associations.<sup>32-37</sup> Thomas et al<sup>7</sup> found that p27 expression in less than 30% of cells on needle biopsy was correlated with high Gleason score and advanced tumor stage. Vis et al<sup>38</sup> reported that p27 expression in less than 50% of cells was the most important clinical determinant of the Gleason score in their study of radical prostatectomy specimens from 81 patients with prostate carcinoma. Although limited numbers of patients and different thresholds have been used in studies, we believe that decreased p27 protein expression is implicated in prostate carcinogenesis, potentially making it a useful adjunct to immunohistochemistry in differentiating benign and malignant lesions as well as predicting histological aggressiveness. We hope that therapeutic avenues for the restoration of p27 function will emerge in prostate carcinoma.

### Author Contributions

Conceptualization: MB; Design and Data collection: GO; Writing: MB, GO; Supervision: MB, GO; Formal analysis: HC.

### Ethics statement

For this study, the approval of the local ethics committee was obtained with the decision 04/04 on 06.03.2018 in the Kırıkkale University Faculty of Medicine.

### ORCID iDs

Özdemir Gülhan  <https://orcid.org/0000-0001-6564-0736>  
Balcı Mahi  <https://orcid.org/0000-0001-5836-2344>

## Supplemental Material

Supplemental material for this article is available online.

## REFERENCES

1. Alinezhad S, Väänänen RM, Ochoa NT, et al. Global expression of AMACR transcripts predicts risk for prostate cancer – a systematic comparison of AMACR protein and mRNA expression in cancerous and noncancerous prostate. *BMC Urol.* 2016;16:10.
2. Dall'Era MA, True LD, Siegel AF, Porter MP, Sherertz TM, Liu AY. Differential expression of CD10 in prostate cancer and its clinical implication. *BMC Urol.* 2007;7:3.
3. Freedland SJ, Seligson DB, Liu AY, et al. Loss of CD10 (neutral endopeptidase) is a frequent and early event in human prostate cancer. *Prostate.* 2003;55:71-80.
4. Tomlins SA, Rhodes DR, Perner S, et al. Recurrent fusion of *TMPRSS2* and *ETS* transcription factor genes in prostate cancer. *Science.* 2005;310:644-648.
5. Hägglöf C, Hammarsten P, Strömvall K, et al. *TMPRSS2*-ERG expression predicts prostate cancer survival and associates with stromal biomarkers. *PLoS ONE.* 2014;9:e86824.
6. Andrews C, Humphrey PA. Utility of ERG versus AMACR expression in diagnosis of minimal adenocarcinoma of the prostate in needle biopsy tissue. *Am J Surg Pathol.* 2014;38:1007-1012.
7. Thomas GV, Schrage MI, Rosenfelt L, et al. Preoperative prostate needle biopsy p27 correlates with subsequent radical prostatectomy p27, Gleason grade and pathological stage. *J Urol.* 2000;164:1987-1991.
8. Epstein JI, Egevad L, Amin MB, et al. The 2014 International Society of Urological Pathology (ISUP) Consensus Conference on Gleason grading of prostatic carcinoma: definition of grading patterns and proposal for a new grading system. *Am J Surg Pathol.* 2016;40:244-252.
9. Marije Hoogland A, Kweldam CF, Van Leenders GLJH. Prognostic histopathological and molecular markers on prostate cancer needle-biopsies: a review. *Nephrourol Mon.* 2016;8:e41505.
10. Jiang Z, Woda BA, Rock KL, et al. P504S: a new molecular marker for the detection of prostate carcinoma. *Am J Surg Pathol.* 2001;25:1397-1404.
11. Rubin MA, Zhou M, Dhanasekaran SM, et al. alpha-Methylacyl coenzyme A racemase as a tissue biomarker for prostate cancer. *JAMA.* 2002;287:1662-1670.
12. Farinola MA, Epstein JI. Utility of immunohistochemistry for alpha-methylacyl-CoA racemase in distinguishing atrophic prostate cancer from benign atrophy. *Hum Pathol.* 2004;35:1272-1278.
13. Murphy AJ, Hughes CA, Lannigan G, Sheils O, O'Leary J, Loftus B. Heterogeneous expression of alpha-methylacyl-CoA racemase in prostatic cancer correlates with Gleason score. *Histopathology.* 2007;50:243-251.
14. Shukla N, Adhya AK, Rath J. Expression of alpha-methylacyl-coenzyme A racemase (AMACR) in colorectal neoplasia. *J Clin Diagn Res.* 2017;11:EC35-EC38.
15. Mah CY, Nassar ZD, Swinnen JV, Butler LM. Lipogenic effects of androgen signaling in normal and malignant prostate [published online ahead of print December 10, 2019]. *Asian J Urol.* doi:10.1016/j.ajur.2019.12.003.
16. Kaur M, Verma S, Gupta R, Pant L, Singh S. CD10 expression pattern in prostatic adenocarcinoma: elucidation of differences between Gleason's grades. *Malays J Pathol.* 2018;40:57-60.
17. Tawfic S, Niehans GA, Manivel JC. The pattern of CD10 expression in selected pathologic entities of the prostate gland. *Hum Pathol.* 2003;34:450-456. doi:10.1016/S0046-8177(03)00077-7.
18. Mishra D, Singh S, Narayan G. Role of B cell development marker CD10 in cancer progression and prognosis. *Mol Biol Int.* 2016;2016:4328697.
19. Wang Z, Wang Y, Zhang J, et al. Significance of the *TMPRSS2*:ERG gene fusion in prostate cancer. *Mol Med Rep.* 2017;16:5450-5458.
20. Liu W. DNA alterations in the tumor genome and their associations with clinical outcome in prostate cancer. *Asian J Androl.* 2016;18:533-542.
21. Font-Tello A, Juanpere N, de Muga S, et al. Association of ERG and *TMPRSS2*-ERG with grade, stage and prognosis of prostate cancer is dependent on their expression levels. *Prostate.* 2015;75:1216-1226.
22. Wang S, Zhang Q, Xu D, et al. Characterize the difference between *TMPRSS2*-ERG and non-*TMPRSS2*-ERG fusion patients by clinical and biological characteristics in prostate cancer. *Gene.* 2018;679:186-194.
23. Lee SL, Yu D, Wang C, et al. ERG Expression in prostate needle biopsy: potential diagnostic and prognostic implications. *Appl Immunohistochem Mol Morphol.* 2015;23:499-505.
24. Nie L, Pan X, Zhang M, et al. The expression profile and heterogeneity analysis of ERG in 633 consecutive prostate cancers from a single center. *Prostate.* 2019;79:819-825.
25. Darnel AD, Lafargue CJ, Vollmer RT, Corcos J, Bismar TA. *TMPRSS2*-ERG fusion is frequently observed in Gleason pattern 3 prostate cancer in a Canadian cohort. *Cancer Biol Ther.* 2009;8:125-130.

26. Fine SW, Gopalan A, Leversha MA, et al. TMPRSS2-ERG gene fusion is associated with low Gleason scores and not with high-grade morphological features. *Mod Pathol*. 2010;23:1325-1333.
27. Mosquera JM, Perner S, Genega EM, et al. Characterization of TMPRSS2-ERG fusion high-grade prostatic intraepithelial neoplasia and potential clinical implications. *Clin Cancer Res*. 2008;14:3380-3385.
28. Kulda V, Topolcan O, Kucera R, et al. Prognostic significance of TMPRSS2-ERG fusion gene in prostate cancer. *Anticancer Res*. 2016;36:4787-4793.
29. Eder IE, Bektic J, Haag P, Bartsch G, Klocker H. Genes differentially expressed in prostate cancer. *BJU Int*. 2004;93:1151-1155.
30. Zhang Z, Rosen DG, Yao JL, Huang J, Liu J. Expression of p14ARF, p15INK4b, p16INK4a, and DCR2 increases during prostate cancer progression. *Mod Pathol*. 2006;19:1339-1343.
31. Viglietto G, Fusco A. Understanding p27kip1 deregulation in cancer: down-regulation or mislocalization? *Cell Cycle*. 2002;1:394-400.
32. Nassif AE, Tãmbara Filho R. Immunohistochemistry expression of tumor markers CD34 and P27 as a prognostic factor of clinically localized prostate adenocarcinoma after radical prostatectomy. *Rev Col Bras Cir*. 2010;37:338-344.
33. Ronen S, Abbott DW, Kravtsov O, et al. PTEN loss and p27 loss differ among morphologic patterns of prostate cancer, including cribriform. *Hum Pathol*. 2017; 65:85-91.
34. Roy S, Singh RP, Agarwal C, Siriwardana S, Sclafani R, Agarwal R. Downregulation of both p21/Cip1 and p27/Kip1 produces a more aggressive prostate cancer phenotype. *Cell Cycle*. 2008;7:1828-1835.
35. Vlachostergios PJ, Karasavvidou F, Kakkas G, et al. Lack of prognostic significance of p16 and p27 after radical prostatectomy in hormone-naïve prostate cancer. *J Negat Results Biomed*. 2012;11:2.
36. Revelos K, Petraki C, Gregorakis A, et al. p27(kip1) and Ki-67 (MIB1) immunohistochemical expression in radical prostatectomy specimens of patients with clinically localized prostate cancer. *In Vivo*. 2005;19:911-920.
37. Sirma H, Broemel M, Stumm L, et al. Loss of CDKN1B/p27Kip1 expression is associated with ERG fusion-negative prostate cancer, but is unrelated to patient prognosis. *Oncol Lett*. 2013;6:1245-1252.
38. Vis AN, van Rhijn BW, Noordzij MA, Schröder FH, van der Kwast TH. Value of tissue markers p27(kip1), MIB-1, and CD44s for the pre-operative prediction of tumour features in screen- detected prostate cancer. *J Pathol*. 2002;197:148-154.